Journal of Power Sources 251 (2014) 370–378

Contents lists available at ScienceDirect

Journal of Power Sources

journal homepage: www.elsevier.com/locate/jpowsour

Including double-layer capacitance in lithium-ion battery mathematical models

N. Legrand [a,b,c], S. Raël [b,*], B. Knosp [a], M. Hinaje [b], P. Desprez [a], F. Lapicque [c]

[a] SAFT, Direction de la Recherche, F-33074 Bordeaux Cedex, France
[b] Université de Lorraine – GREEN, F-54518 Vandoeuvre-lès-Nancy Cedex, France
[c] Université de Lorraine – LRGP, F-54001 Nancy, France

HIGHLIGHTS

- We include double layer capacitance in a mathematical model of lithium-ion battery.
- We demonstrate that the usual model formulation leads to a physical error.
- We develop a new formulation suitable for double layer capacitance implementation.
- We compare the two model formulations with double layer capacitance.
- We determinate conditions for which significant differences are obtained.

ARTICLE INFO

Article history:
Received 19 July 2013
Received in revised form
12 September 2013
Accepted 9 November 2013
Available online 28 November 2013

Keywords:
Lithium-ion battery
Electrochemical dynamic modeling
Mass and charge transport
Double layer capacitance

ABSTRACT

A fundamental model of lithium-ion battery cell based on Newman's works is presented in this article, including migration and diffusion of species and charges in electrodes and electrolyte. The particularity of our work is that the double layer capacitance, which is commonly neglected, is integrated in the model. We especially emphasize how to include correctly, in a physical point of view, the double layer capacitance in the electrochemical lithium-ion cell model. It is first demonstrated that the widely used mathematical formulation of the model leads to a physical error when the double layer capacitance is included, and a new formulation free of this error is proposed. Then are given the conditions for which the physical error mentioned before may cause appreciable inaccuracy in the prediction. Simulations have been carried out to validate the present analysis, and the results obtained show that the difference in cell voltage can attain several tens of millivolts.

1. Introduction

Numerous mathematical models have formerly been developed in order to describe locally migration and diffusion phenomena involved in a lithium-ion cell through coupled partial differential equations (PDE) involving space and time. One of the earlier studies [1,2] led to one-dimensional models widely used nowadays, and was recently improved by some other studies introducing thermal considerations [3,4]. However, the double layer phenomenon is very frequently ignored in this kind of model, although it can be of great importance to be integrated, especially in a system approach, or for energy losses calculation when batteries are coupled with power electronics converters.

This article is focused on including electric double-layer phenomenon in an electrochemical model of lithium-ion battery cell. This model is based on the 1-D mathematical representation of charge and mass transport phenomena in electrodes and electrolyte developed in Newman's works [1,2]. In the first part, mass and charge transport equations, electrochemical kinetic equations, and boundary conditions of the lithium-ion battery model are briefly reminded. Then emphasis is put on the definition of electrolyte potential. In particular, it is demonstrated that the usual formulation of the model, which is of course fundamentally based on a local definition for this potential, is however expressed versus an electrolyte potential considered at the average electrolyte concentration. We propose an alternative and equivalent formulation of the model, which explicitly takes into account the local electrolyte concentration to calculate the electrolyte potential. The second part of the paper explains how to include the double layer capacitance in mathematical models for lithium-ion cells: we demonstrate here

* Corresponding author. Tel.: +33 383 59 56 54; fax: +33 383 59 56 53.
E-mail address: Stephane.Rael@univ-lorraine.fr (S. Raël).

0378-7753/$ – see front matter © 2013 Elsevier B.V. All rights reserved.
http://dx.doi.org/10.1016/j.jpowsour.2013.11.044

that using the usual formulation of the lithium-ion cell model, as done like in Ref. [5], leads to a physical error in the calculation of the capacitive current contribution. Parameter conditions for which this physical error causes significant inaccuracy are determined by equation analysis. Comparison between the usual formulation of the lithium-ion cell model, and the present formulation relying upon thorough physical equations, is finally presented.

2. Mathematical 1D model of lithium-ion batteries

As depicted in Fig. 1, a lithium-ion cell is composed of two composite electrodes, the electrolyte, a porous separator, and two current collectors. The active material of the positive electrode is usually a transition metal oxide containing lithium, such as cobalt ($LiCoO_2$) or nickel ($LiNiO_2$) oxide, or iron phosphate ($LiFePO_4$), or NMC materials ($LiNi_yMn_zCo_{1-y-z}O_2$). The insertion material of the negative electrode is a carbon material of coke type, graphite, or amorphous carbon. The electrolyte, in which a lithium salt e.g., lithium hexafluorophosphate $LiPF_6$ is dissolved, ensures ion transport within the battery. The separator is an electronic insulator which allows to avoid short circuit between the electrodes. It must be porous to allow ion transport between the electrodes. In lithium-ion technology, it usually contains polyethylene (PE) and/or polypropylene (PP).

Lithium-ion batteries operate according to the "rocking chair" principle [6]: during operation, lithium ions Li^+ leave the first electrode structure, migrate within the electrolyte, and insert into the second electrode structure. The equations associated with insertion–extraction phenomenon of lithium ions in electrode materials are, at the negative electrode:

$$Li_{y+dy}C_6 \underset{\text{charge}}{\overset{\text{discharge}}{\rightleftharpoons}} Li_yC_6 + dy\cdot Li^+ + dy\cdot e^- \quad (1)$$

and at the positive electrode:

$$Li_zMO_2 + dz\cdot Li^+ + dz\cdot e^- \underset{\text{charge}}{\overset{\text{discharge}}{\rightleftharpoons}} Li_{z+dz}MO_2 \quad (2)$$

Coefficients y and z, with $(0 < y < 1)$ and $z\ (0 < z < 1)$, are the lithium insertion rates in the negative and the positive electrodes, respectively.

In this section, it is first reminded the mathematical lithium-ion battery model introduced by Doyle et al. for metal lithium cells [1], and later for dual lithium ion insertion cells [2]. This model was recently improved by Smith and Wang by experimental validation in Ref. [7], and by thermal modeling in Ref. [3]. Then, an equivalent formulation of the model is presented. However in the present work, the local electrolyte concentration has been explicitly taken into account for calculation of the electrolyte potential, whereas in the usual formulation developed in the above cited works, equation transformations (detailed in Section 2.3) leads to introduce an electrolyte potential defined at the average electrolyte concentration.

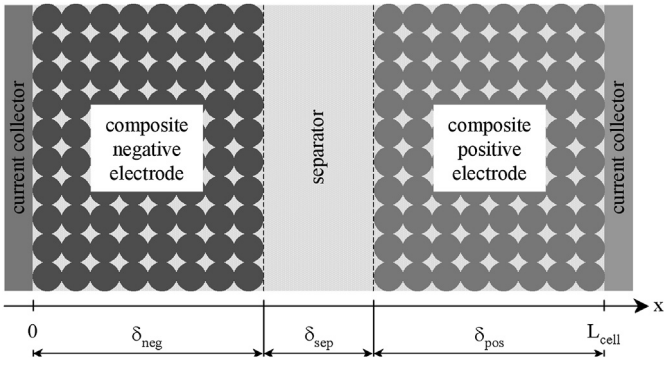

Fig. 1. 1-D model of the lithium-ion cell.

2.1. Assumptions and unknowns

Fig. 1 presents the three domains of the 1D lithium-ion cell model: the composite negative electrode containing Li_yC_6 particles, the separator – a porous dielectric ensuring electronic insulation and ion migration –, and the composite positive electrode containing Li_zMO_2 particles. The electrode structure is impregnated with electrolyte. The model formulation is based on the following assumptions:

1) the cell temperature is constant and uniform throughout the cell,
2) in the electrolyte phase, mass and charge transports are respectively due to diffusion after Fick's law and migration after Ohm's law, along the x direction in Fig. 1. Convection is neglected,
3) in the solid phase, lithium transport is caused by diffusion expressed using Fick's law and is treated spherical: the active material particles are supposed to be monodisperse spheres. Particle radius is considered small enough compared with the thickness of both electrodes, so that the lithium concentration at solid/electrolyte interface could be computed as a continuous function of space variable x. Electron transport through migration (Ohm's law) is one-dimensional along the x direction in Fig. 1.

Four physical variables have been accounted for in the model:

1) the ionic concentration c_e of the electrolyte,
2) the lithium concentration c_s in active material particles,
3) the electrolyte phase potential ϕ_e,
4) the solid phase potential ϕ_s.

Electrolyte phase variables c_e and ϕ_e can be defined in the three domains, whereas solid phase variables c_s and ϕ_s are only in the electrode domains. As mentioned before, in the model formulation commonly used in the literature, electrolyte potential ϕ_e is calculated at the average electrolyte concentration, corresponding to the OCV measurement conditions.

2.2. Usual model formulation

The usual model formulation has been presented in Ref. [8]. Table 1 hereafter summarizes transport and conservation equations

Table 1
1D electrochemical model equations.

Unknown	Partial differential equations	Boundary conditions
c_s	$\begin{cases} \varphi_s(r) = -D_s\cdot\frac{\partial c_s(r)}{\partial r} \\ \frac{\partial c_s(r)}{\partial t} = \frac{1}{r^2}\cdot\frac{\partial}{\partial r}\left(D_s\cdot r^2\cdot\frac{\partial c_s(r)}{\partial r}\right) \end{cases}$	$\begin{cases} \varphi_s(0) = 0 \\ \varphi_s(R_s) = \frac{j^{Li}(x)}{a_s\cdot F} \end{cases}$
ϕ_s	$\begin{cases} J_s(x) = -\sigma_{s,eff}\cdot\frac{\partial\phi_s(x)}{\partial x} \\ \frac{\partial J_s(x)}{\partial x} = -j^{Li}(x) \end{cases}$	$\begin{cases} J_s(0) = I_{cell}/A_{cell} \\ J_s(\delta_{neg}) = 0 \\ J_s(L_{cell}-\delta_{pos}) = 0 \\ J_s(L_{cell}) = I_{cell}/A_{cell} \end{cases}$
c_e	$\varepsilon_e\cdot\frac{\partial c_e(x)}{\partial t} = \frac{\partial}{\partial x}\left(D_{e,eff}\cdot\frac{\partial c_e(x)}{\partial x}\right) + (1-t_p)\cdot\frac{j^{Li}(x)}{F}$	$\begin{cases} \frac{\partial c_e}{\partial x}(0) = 0 \\ \frac{\partial c_e}{\partial x}(L_{cell}) = 0 \end{cases}$
ϕ_e	$\begin{cases} J_e(x) = -\sigma_{e,eff}(x)\cdot\frac{\partial\phi_e(x)}{\partial x} - \sigma_{De,eff}(x)\cdot\frac{\partial\ln(c_e(x))}{\partial x} \\ \frac{\partial J_e(x)}{\partial x} = j^{Li}(x) \end{cases}$	$\begin{cases} \frac{\partial\phi_e}{\partial x}(0) = 0 \\ \frac{\partial\phi_e}{\partial x}(L_{cell}) = 0 \end{cases}$

of the 1-D electrochemical lithium-ion cell model. In these equations, j^{Li} is the volume rate of Li^+ current generation (in A m^{-3}), determined by Butler–Volmer kinetics law as follows:

$$j^{Li}(x) = a_s \cdot j_0 \cdot \left(\exp\left(\alpha_o \frac{\eta(x)}{u_T} \right) - \exp\left(-\alpha_r \frac{\eta(x)}{u_T} \right) \right), \quad (3)$$

with j_0 the exchange current density, a_s the electrode active surface per electrode volume unit, η the local interface overvoltage, u_T the thermal voltage ($u_T = RT/F$, R being the gas constant, T the temperature, and F the Faraday's constant), α_o and α_r the oxidation and reduction transfer coefficients, respectively. Electrode particles being supposed spherical, ratio a_s can be expressed versus particle radius, R_s, and active material volume fraction, ε_s, by:

$$a_s = \frac{3\varepsilon_s}{R_s}. \quad (4)$$

The effective electronic conductivity $\sigma_{s,eff}$ depends on the electrode conductivity, σ_s, and the active material volume fraction ε_s:

$$\sigma_{s,eff} = \varepsilon_s \cdot \sigma_s \quad (5)$$

The effective salt diffusion coefficient $D_{e,eff}$, and the effective ionic conductivity $\sigma_{e,eff}$ of the electrolyte are given by Bruggeman's relation [9]:

$$\begin{cases} D_{e,eff} = \varepsilon_e^{\beta} \cdot D_e \\ \sigma_{e,eff} = \varepsilon_e^{\beta} \cdot \sigma_e \end{cases}, \quad (6)$$

where β is the Bruggeman's exponent, D_e is the salt diffusion coefficient in the electrolyte phase, and σ_e is electrolyte ionic conductivity. For this last parameter, which depends on the electrolyte concentration c_e, the empirical law proposed in Ref. [3] has been used:

$$\sigma_e(x) = 0.00158 \cdot c_e(x) \cdot \exp\left(-5.363 \cdot 10^{-5} \cdot c_e^{1.4}(x) \right). \quad (7)$$

The model formulation commonly used in the literature involves an electrolyte potential ϕ_e defined at the average electrolyte concentration. As a result, the local electrode overvoltage involved in the j^{Li} expression (Eq. (3)) is written as:

$$\eta(x) = (\phi_s(x) - \phi_e(x)) - U(x), \quad (8)$$

where the interfacial equilibrium voltage U only depends on the lithium insertion rate at the surface of solid phase particles, i.e., on the ratio $c_{s,e}(x)/c_{smax}$ between lithium concentration at $r = R_s$ and maximum lithium concentration in solid phase. The variations of potential U with the lithium insertion rate plotted in Fig. 2, has been determined by means of empirical formula given in Ref. [3]. As a matter of fact, as demonstrated in the next section, in the usual model formulation the theoretical effect of the local electrolyte concentration on electrochemical kinetics is implicitly included in ϕ_e definition, and in the expression of the effective diffusional ionic conductivity $\sigma_{De,eff}$, which is given in this case by:

$$\sigma_{De,eff} = 2 \cdot u_T \cdot (t_p - 1) \cdot \sigma_{e,eff}. \quad (9)$$

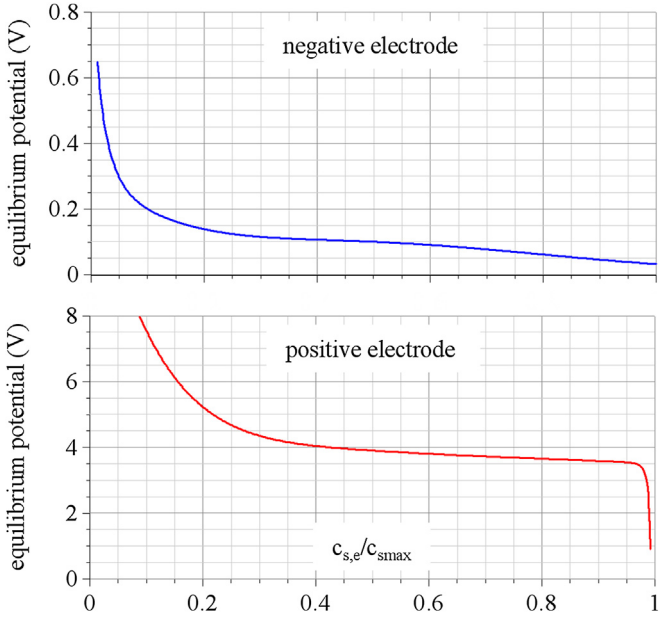

Fig. 2. Electrode equilibrium potentials versus lithium insertion rate.

2.3. Model formulation with explicit electrolyte concentration effect

In the following formulation, the actual electrolyte potential ϕ_e, defined at the local electrolyte concentration, is considered. The total ion current density $\vec{J}_e$ associated with ion transport in the electrolyte phase is the sum of two conduction components for potential gradient-induced migration of anion and cation and two diffusion terms for anion and cation transport:

$$\begin{cases} \vec{J}_e = \vec{J}_n + \vec{J}_p \\ \vec{J}_n = -\sigma_n \cdot \mathrm{grad}(\phi_e) + \sigma_n \cdot u_T \cdot \mathrm{grad}(\ln(c_e)) \\ \vec{J}_p = -\sigma_p \cdot \mathrm{grad}(\phi_e) - \sigma_p \cdot u_T \cdot \mathrm{grad}(\ln(c_e)) \end{cases}, \quad (10)$$

where $\vec{J}_n$ and $\vec{J}_p$ are the anion and cation current densities, and σ_n and σ_p are the anion and cation conductivities of the electrolyte, respectively. The overall set of equations results in:

$$\vec{J}_e = -\sigma_e \cdot \mathrm{grad}(\phi_e) + (\sigma_n - \sigma_p) \cdot u_T \cdot \mathrm{grad}(\ln(c_e)), \quad (11)$$

where σ_e is the electrolyte ionic conductivity:

$$\sigma_e = \sigma_n + \sigma_p. \quad (12)$$

It should be noticed here that conduction components of $\vec{J}_e$ are added, while diffusion components are subtracted. In particular, if anion and cation diffusion coefficients are equal (i.e., if $\sigma_n = \sigma_p$, taking into account Einstein's relation), the total diffusion component is zero, and the total ion current density in the electrolyte is purely ohmic. Introducing the cation transference number $t_p = \sigma_p/\sigma_e$, the total ion current density in the electrolyte can be expressed versus potential ϕ_e and concentration c_e as in Table 1:

$$\vec{J}_e = -\sigma_e \cdot \mathrm{grad}(\phi_e) - \sigma_{De} \cdot \mathrm{grad}(\ln(c_e)), \quad (13)$$

but with a different expression for the diffusional ionic conductivity than in the case of the formulation commonly used in the literature (Eq. (9)):

$$\sigma_{De} = 2 \cdot u_T \cdot \left(t_p - \frac{1}{2} \right) \cdot \sigma_e. \quad (14)$$

Through this relation, which can be found for instance in Ref. [10] in the presentation of Planck–Henderson equation, it can easily be deduced the following physical evidence. In a 1:1 binary ionic solution, for which the diffusion coefficients of the two ions are assumed equal – corresponding to $t_p = 1/2$ – local

electroneutrality implies that a concentration gradient produces identical specific fluxes, and therefore opposite diffusion current densities, resulting in a global diffusion current density equal to zero.

Eq. (9) can be established by considering the Nernst relation between the actual electrolyte potential ϕ_e, calculated at the local electrolyte concentration, and the electrolyte potential $\phi_{e,mean}$ used in the widespread formulation, with reference to the average electrolyte concentration:

$$\phi_e = \phi_{e,mean} - u_T \cdot \ln\left(\frac{c_e}{c_{e,mean}}\right). \quad (15)$$

As a matter of fact, inserting this relation in Eq. (13) yields the charge transport equation that is usually given in the literature:

$$\vec{J}_e = -\sigma_e \cdot \mathrm{grad}(\phi_{e,mean}) - 2 \cdot u_T \cdot (t_p - 1) \cdot \sigma_e \cdot \mathrm{grad}(\ln(c_e)). \quad (16)$$

The difference in the model formulation does not solely concern the modified expression of the diffusional ionic conductivity in the expression of $\vec{J}_e$ when the actual electrolyte potential is used, as explained below. As a matter of fact, the local electrolyte concentration has to be taken into account in the local OCV calculation, according to Nernst law. As a result, the local electrode overvoltage involved in the j^{Li} expression (Eq. (3)) is equal to:

$$\eta = (\phi_s - \phi_e) - \left(U + u_T \cdot \ln\left(\frac{c_e}{c_{e,mean}}\right)\right), \quad (17)$$

which is equivalent to the usual formulation expression (Eq. (8)), i.e., with notations used in this section:

$$\eta = (\phi_s - \phi_{e,mean}) - U. \quad (18)$$

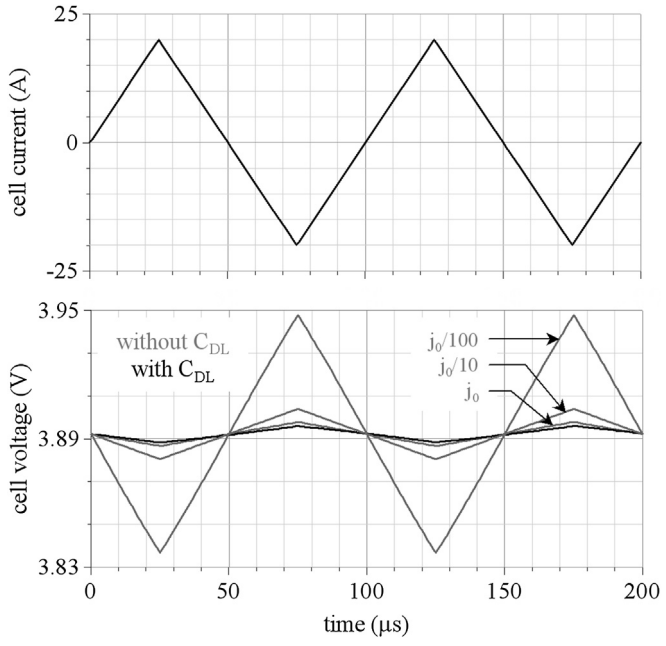

Fig. 3. Typical current waveform generated by power electronic converters, and related cell voltage responses. Simulation carried out with Smith and Wang's model parameters [3], except for the exchange current density: $j_{0,neg}$ = 3.6 A m^2 and $j_{0,pos}$ = 2.6 A m^2 for "j_0/10" curve, $j_{0,neg}$ = 0.36 A m^2 and $j_{0,pos}$ = 0.26 A m^2 for "j_0/100" curve. Initial SOC: 100%, temperature: 300 K, double layer capacitance: 20 µF cm^{-2}, switching frequency: 10 kHz.

2.4. Summary

In this section, two formulations of the same 1-D electrochemical model of lithium-ion cell have been presented, both described by partial differential equations and boundary conditions given in Table 1. The first, introduced by Doyle et al. [1,2,11], is nowadays commonly employed, in particular by Smith et al. [3,7,12], White et al. [4,13], Verbrugge et al. [14], Bernardi and Gob [15]. This formulation is expressed versus an electrolyte potential defined at the average electrolyte concentration, corresponding to the OCV measurement conditions. As a result, the OCV considered for calculation of the local electrode overvoltage is the interfacial equilibrium voltage U, the effect of the local electrolyte concentration on electrochemical kinetics being included in the definition of the effective diffusional ionic conductivity. These two variables are thus given by:

$$\begin{cases} \mathrm{OCV}(x) = U(x) \\ \sigma_{De,eff}(x) = 2 \cdot u_T \cdot (t_p - 1) \cdot \sigma_{e,eff}(x) \end{cases}. \quad (19)$$

The second formulation, introduced in this work, is expressed versus the actual electrolyte potential, with reference to local electrolyte concentration. Then, the OCV considered for calculation of the local electrode overvoltage takes into account the effect of the local electrolyte concentration through Nernst law, and the effective diffusional ionic conductivity does not have to be corrected:

$$\begin{cases} \mathrm{OCV}(x) = U(x) + u_T \cdot \ln\left(\frac{c_e(x)}{c_{e,mean}}\right) \\ \sigma_{De,eff}(x) = 2 \cdot u_T \cdot \left(t_p - \frac{1}{2}\right) \cdot \sigma_{e,eff}(x) \end{cases}. \quad (20)$$

Important: as demonstrated before, these two formulations are mathematically equivalent, and their computation with Comsol Multiphysics® actually shows no numerical difference.

When computing the model, the usual formulation can be preferable, as far as it avoids the logarithm function in the OCV definition, which is numerically an advantage. However, a physical problem appears when the double layer capacitance has to be included in this lithium-ion cell model. The related capacitive current density depends indeed on the derivative of the interfacial voltage $\phi_s - \phi_e$, which requires the actual electrolyte potential.

3. Modeling double layer capacitance

Abundant works have been devoted to fundamentally based models but only a few also integrate the double layer capacitance, which is neglected in most cases. However, describing electric double-layer phenomenon is necessary for system applications, for which short-time effects are essential. As a matter of fact, in many applications e.g., uninterruptible power supplies, or board networks in transportation, batteries are often connected to power electronic converters as a link – or energy buffer – to other sources e.g., industrial grid, fuel cells, photovoltaic generators, wind turbines, or to variable loads e.g., electrical motors. For safety reasons, these converters are usually current controlled by high dynamic regulators, with a response time to a step lower than 10 ms. Therefore, accurate knowledge of the battery resistive and capacitive behaviors at high frequency i.e., above a few hundred Hertz is required to calculate with accuracy regulator parameters and stability margins of the system. Moreover, power electronic converters generate battery current ripples at switching frequency, so that RMS and mean currents may significantly differ from each other, especially at low mean current level. Therefore an appropriate model including double layer capacitance is required to

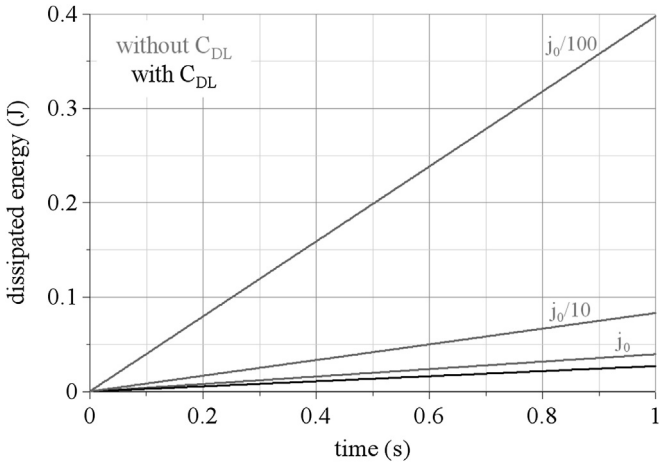

Fig. 4. Losses in floating conditions. Simulation carried out with Smith and Wang's model parameters [3] for a 6 Ah battery, except for exchange current: $j_{0,neg} = 3.6$ A m^2 and $j_{0,pos} = 2.6$ A m^2 for "j_0/10" curve, $j_{0,neg} = 0.36$ A m^2 and $j_{0,pos} = 0.26$ A m^2 for "j_0/100" curve. Initial SOC: 100%, temperature: 300 K, double layer capacitance: 20 μF cm^{-2}, switching frequency: 10 kHz.

determine accurately battery energy losses in power electronic applications.

Figs. 3 and 4 present simulation results obtained with the mathematical lithium-ion cell model detailed in the previous section. To introduce typical current waveforms generated by power electronic converters, this model has been implemented in Saber®, a simulation software widely used in electrical engineering, by means of an electrical analogy to describe migration and diffusion of species and charges within the cell. The implementation method is described in Ref. [8]. Table 2 provides the geometry, concentration and physical parameters required for the model simulation: these values coming from Ref. [3] are related to a 6 Ah lithium-ion cell. Fig. 3 shows the typical triangular current waveform induced by power electronic conversion system with a switching frequency of 10 kHz, and the cell voltage response depending on whether the double layer capacitance is taken into account or not. A parametric study has been carried out on the exchange current density, in order to emphasize the effect of double layer capacitance on cell voltage response. It can be noticed here that the values used for the exchange current density in Smith and Wang's work [3] are large, around one order of magnitude [16], or even more [17], higher than that used in some works. As expected, it can be observed that including double layer capacitance decreases the "high frequency" resistance. Indeed, this resistance is only due to charge transport losses in electrodes and electrolyte, whereas electrochemical losses also contribute to define the electrical behavior at high frequencies, when the double layer capacitance is ignored.

Table 2
Smith and Wang's model parameters [3].

Parameter	Negative electrode	Separator	Positive electrode
Thickness δ [μm]	50	25.4	36.4
Particle radius R_s [μm]	1	–	1
Solide phase volume fraction solide ε_s [−]	0.580	–	0.500
Electrolyte phase volume fraction ε_e [−]	0.332	0.500	0.330
Cell area A_{cell} [m^2]	1.0452	1.0452	1.0452
Max solid phase conc. c_{smax} [mol dm^{-3}]	16.1	–	23.9
Insertion rate $c_{s,e}/c_{smax}$ at SOC = 0% [−]	0.216	–	0.936
Insertion rate $c_{s,e}/c_{smax}$ at SOC = 100% [−]	0.676	–	0.442
Average electrolyte conc. $c_{e,mean}$ [mol dm^{-3}]	1.2	1.2	1.2
Exchange current density j_0 [A m^2]	36	–	26
Oxydation transfer coefficient α_a [−]	0.5	–	0.5
Reduction transfer coefficient α_r [−]	0.5	–	0.5
Solid phase Li diffusion coeff. D_s [m^2 s^{-1}]	2×10^{-16}	–	3.7×10^{-16}
Electronic conductivity σ_s [S m^{-1}]	100	–	10
Electrolyte phase diffusion coeff. D_e [m^2 s^{-1}]	2.6×10^{-10}	2.6×10^{-10}	2.6×10^{-10}
Electrolyte ionic conductivity σ_e [S m^{-1}]	Eq. (7)	Eq. (7)	Eq. (7)
Bruggeman's exponent β [−]	1.5	1.5	1.5
Li^+ transference number t_p [−]	0.363	0.363	0.363
Double layer capacitance C_{DL} [F m^{-2}]	0.2	–	0.2

The RMS value of a triangular current waveform is given versus its mean value I_{MEAN} and its current ripple amplitude Δi by:

$$I_{RMS,tri} = I_{MEAN} \cdot \sqrt{1 + \frac{\Delta i^2}{12 \cdot I_{MEAN}^2}}. \quad (21)$$

Therefore, the contribution of current ripples in ohmic losses increases when the mean current decreases. For this reason, Fig. 4 presents simulation results related to losses in floating voltage conditions, i.e., with zero mean current. In the example treated here and with Smith and Wang's model parameters [3], losses are about 1.5 times higher if the double layer capacitance is ignored. This figure depends of course on activation losses, thus on exchange current densities. With exchange current densities lower of one order of magnitude, the ratio becomes about 3, and nearly 15 with exchange current densities lower of two orders of magnitude.

This section is aimed at explaining how to include the double layer capacitance in the mathematical lithium-ion cell model detailed in Section 2, as done in Ref. [5]. Then, we emphasize the theoretical physical importance of the electrolyte potential definition.

3.1. Including double layer capacitance in lithium-ion mathematical model [5]

In a rigorous manner, the current density at the electrolyte/solid active material interface has faradaic and non-faradaic current contributions. The second contribution is related to the transient change in charge state of the double layer capacitance, and is expressed in A m^{-3} as:

$$j^{DL}(x) = a_s \cdot C_{DL} \cdot \frac{\partial(\phi_s(x) - \phi_e(x))}{\partial t}, \quad (22)$$

where C_{DL} is the surface double layer capacitance (F m^{-2}) exhibited at the electrolyte/solid active material interface. In positive and negative electrodes, charge conservation equations including the double layer contribution can be established, as shown schematically in Fig. 5. This leads to:

$$\begin{cases} J_s(x) = J_s(x + dx) + j^{Li}(x) \cdot dx + j^{DL}(x) \cdot dx \\ J_e(x + dx) = J_e(x) + j^{Li}(x) \cdot dx + j^{DL}(x) \cdot dx \end{cases}, \quad (23)$$

what can be locally expressed in the form:

$$\begin{cases} \frac{\partial J_s(x)}{\partial x} = -\left(j^{Li}(x) + j^{DL}(x)\right) \\ \frac{\partial J_e(x)}{\partial x} = +\left(j^{Li}(x) + j^{DL}(x)\right) \end{cases}. \quad (24)$$

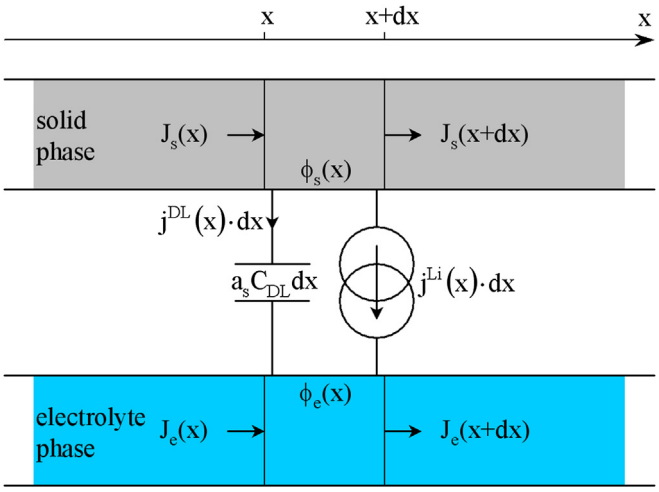

Fig. 5. Schematic representation of local charge conservation in both electrodes, including the double layer current contribution.

3.2. About lithium-ion cell model formulations

In Eq. (22), the electrolyte potential is necessarily defined with reference to local electrolyte concentration, and not to mean concentration. As a result, using the widespread formulation of lithium-ion cell model when implementing the double layer capacitance, as in Ref. [5], is not physically totally consistent, and can theoretically lead to small inaccuracy. In effect, when relation (15) between ϕ_e and $\phi_{e,mean}$ (cf. Section 2.3) is introduced in Eq. (22), the double layer current contribution can be written as:

$$j^{DL}(x) = a_s \cdot C_{DL} \cdot \frac{\partial\left(\phi_s(x) - \phi_{e,mean}(x)\right)}{\partial t} + a_s \cdot C_{DL} \cdot \frac{u_T}{c_e(x)} \cdot \frac{\partial c_e(x)}{\partial t}. \tag{25}$$

Only the first term is taken into account in the usual formulation. It will be shown in the next section that the second term is often negligible, so that the two formulations give very similar results. However, for specific conditions that lead to a drastic decrease in the electrolyte concentration near the cell current collectors ($x = 0$ or $x = L_{cell}$, according to Fig. 1), a significant difference between the two formulations may appear, resulting in cell voltage differences of up to 50–100 mV.

4. Focusing on the differences between the two formulations

In what follows, the subscript "mean" is employed to identify variables specifically associated with the commonly used model formulation, expressed versus an electrolyte potential defined at the average electrolyte concentration. No particular subscript is employed for the formulation introduced in this work, expressed versus the actual electrolyte potential, calculated at the local electrolyte concentration. As mentioned before, capacitive current contributions can be expressed in A m^{-3} as:

$$\begin{cases} j^{DL}(x) = a_s \cdot C_{DL} \cdot \frac{\partial(\phi_s(x) - \phi_e(x))}{\partial t} \\ j^{DL}_{mean}(x) = a_s \cdot C_{DL} \cdot \frac{\partial\left(\phi_s(x) - \phi_{e,mean}(x)\right)}{\partial t} \end{cases}, \tag{26}$$

the difference between these two contributions being:

$$j^{DL}_{mean}(x) - j^{DL}(x) = -a_s \cdot C_{DL} \cdot \frac{u_T}{c_e(x)} \cdot \frac{\partial c_e(x)}{\partial t}. \tag{27}$$

Thus, the discrepancy between the two formulations relies on the electrolyte local concentration. More precisely, according to Eq. (27), a significant error can be observed in case that the electrolyte concentration attains locally very low levels.

We study hereafter the conditions to obtain appreciable differences between the two models for the electric double layer in lithium-ion batteries. For this purpose, the 1D mathematical model of lithium-ion battery described in Section 2 has been implemented in a numerical code for multiphysics modeling (Comsol Multiphysics®). Finite element method was used, each domain was discretized in 40 elements. Simulation results presented in this section have been obtained by using geometry, concentration and physical parameters extracted from Smith and Wang's work [3] and detailed in Table 2. These parameters are associated with a lithium-ion cell, the capacity of which is 6 Ah.

4.1. Differences between the two model formulations for short times

The electrolyte concentration is a state variable that cannot vary quickly – in comparison with electrical variables – therefore it cannot be considered to decrease to zero within a few milliseconds. Thus, one can predict that there is nearly no difference in short times between the two capacitive currents of Eq. (26): this means that the two lithium-ion battery model formulations are almost equivalent in short times, whatever the conditions of use.

For illustration, Fig. 6 presents the relative difference obtained on capacitive currents at the positive electrode terminal (i.e., $(j^{DL} - j^{DL}_{mean})/j^{DL}$ at $x = L_{cell}$) during the first 10 ms of a high rate discharge, here 20 C. This regime has been simulated with different values for the double layer capacitance C_{DL}, and for the electronic conductivity $\sigma_{s,pos}$ of the positive electrode. It has been checked that the electrolyte phase diffusion coefficient D_e had no influence in short times. The capacitive current gap does not exceed 1% at $t = 10$ ms, which is not significant. Consequently, the resulting difference in cell voltage at $t = 10$ ms is calculated to be less than 10 μV.

Therefore, we can conclude that for the description of "high frequency" effects, the two formulations are almost identical. This is not always the case in long times, over a couple of seconds.

4.2. Differences between the two model formulations for long times

For long times and particular conditions, electrolyte concentration may decrease to very low values. Such situation can occur

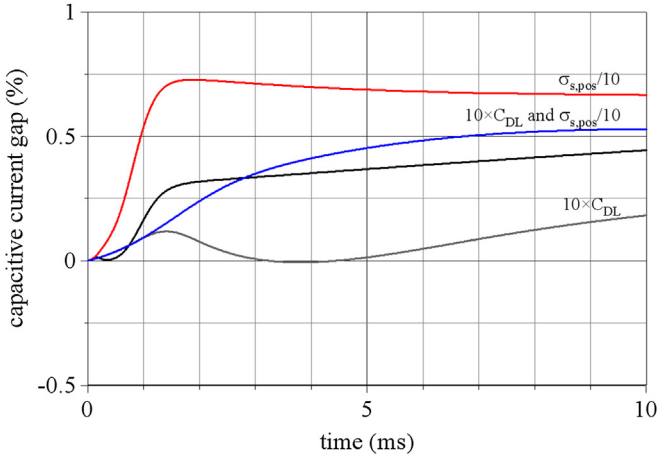

Fig. 6. Simulation of a 20 C discharge: capacitive current gap in short times at positive electrode terminal (initial SOC: 100%, temperature: 300 K, curve in black: Smith and Wang's parameters [3], others curves: Smith and Wang's parameters except for given parameter values).

when two conditions are met: (i) high rate regime, and (ii) low electrolyte phase diffusion coefficient.

Profiles of electrolyte concentration first depend on the current level and the working regime i.e., charge or discharge. For a constant current discharge, the electrolyte concentration will be greater than the mean concentration $c_{e,mean}$ in the negative electrode where lithium ions are extracted, and lower than $c_{e,mean}$ in the positive electrode where lithium ions are inserted. Obviously the reverse situation is encountered at constant current charge. At the beginning of the discharge, if the electrode effective electronic conductivity $\sigma_{s,eff}$ is higher than the electrolyte effective conductivity $\sigma_{e,eff}$, the electrochemical reaction takes place preferentially near the separator, at $x = \delta_{neg}$ and $x = L_{cell} - \delta_{pos}$, according to Fig. 1. This property has been demonstrated in Refs. [18] and [1]. Thus, in the case treated here, one can first observe electrolyte concentration optima (maximum for the negative electrode, minimum for the positive electrode) near the separator. During the discharge, the location of these optima moves slowly toward the cell current collectors ($x = 0$ and $x = L_{cell}$, according to Fig. 1), where ion flows are zero. Fig 7 gives as an illustrating example the time variation of the electrolyte concentration profiles within the lithium-ion cell, for a discharge at 120 A (20 C rate). It can be also observed that, as expected, a high rate regime does not suffice to obtain low values for electrolyte concentration. As a result, the cell voltage gap is lower than 1 mV throughout the 20 C discharge.

A parameter which greatly influences the electrolyte concentration profile is the electrolyte phase diffusion coefficient D_e. Fig. 8 presents for example the same simulation as previously, but carried out with $D_e/10$ (in comparison with Smith and Wang's value [3]). With such a value, at a high rate discharge regime, electrolyte concentration decreases down to zero at the positive electrode terminal. We obtain here conditions, i.e., high current rate and low electrolyte phase diffusion coefficient, for which the two formulations of lithium-ion battery model including double layer capacitance can exhibit significant differences.

Indeed, for such conditions and as shown in Fig. 9, the additional term in capacitive current j^{DL} (cf. Eq. (25) or Eq. (27)) can represent an important part of j^{DL}, and can even be greater in absolute value than j^{DL}. In the example shown in Fig. 9, this situation occurs for $t = 19.5$ s. This clearly means that capacitive behaviors associated with the two formulations become opposite at positive electrode terminal, i.e., at $x = L_{cell}$. As a matter of fact it can be observed in Fig. 10 that the capacitive voltage $\phi_s(L_{cell}) - \phi_e(L_{cell})$ given by our model formulation goes on decreasing during discharge after $t = 19.5$ s, whereas the capacitive voltage $\phi_s(L_{cell}) - \phi_{e,mean}(L_{cell})$ of the usual model formulation begins to increase during discharge for $t > 19.5$ s, which has no physical reality.

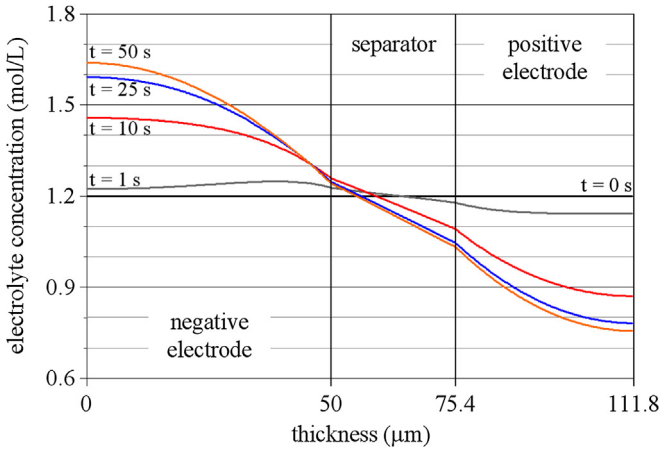

Fig. 7. Simulation of a 20 C discharge: electrolyte concentration profile within the cell (initial SOC: 100%, temperature: 300 K).

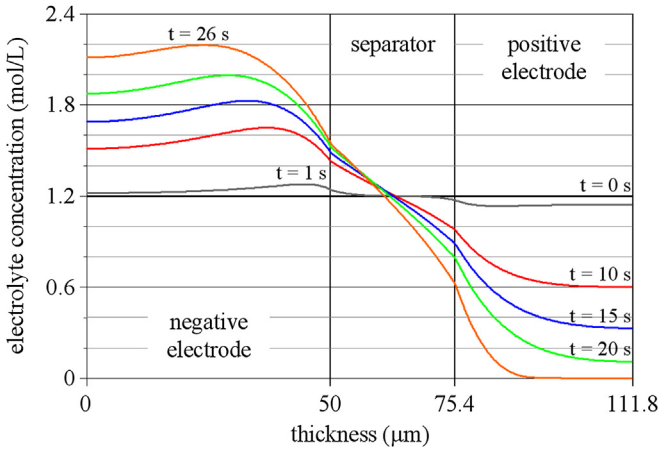

Fig. 8. Simulation of a 20 C discharge: electrolyte concentration profile within the cell (electrolyte phase diffusion coefficient: $D_e = 2.6 \times 10^{-10}/10$ m^2 s^{-1}, initial SOC: 100%, temperature: 300 K).

This results in a cell voltage gap between the two formulations that can become somewhat significant, at several tens of millivolts. Fig. 11 shows the evolution of this cell voltage gap in the extreme case treated here (20 C rate discharge, electrolyte phase diffusion coefficient tenfold lower than Smith and Wang's value [3]). The gap reaches 50 mV at the end of the simulation occurring at $t = 27.1$ s, time for which the value zero for the electrolyte concentration gives rise to computation error.

To conclude, it should be noticed that the low values used for the electrolyte phase diffusion coefficient to emphasize the discrepancies between the formulations of the lithium-ion cell model are not only theoretical, but also practical. Indeed, such values can be obtained at low temperature, as demonstrated in an experimental study of Valoen and Reimers [19] on transport properties of electrolyte employed in lithium-ion technology. In this work, the electrolyte phase diffusion coefficient is divided by 14 if temperature decreases from 333 K to 262 K, and the value at 262 K, of about 5×10^{-11} m^2 s^{-1}, is in the order of magnitude of the value used here.

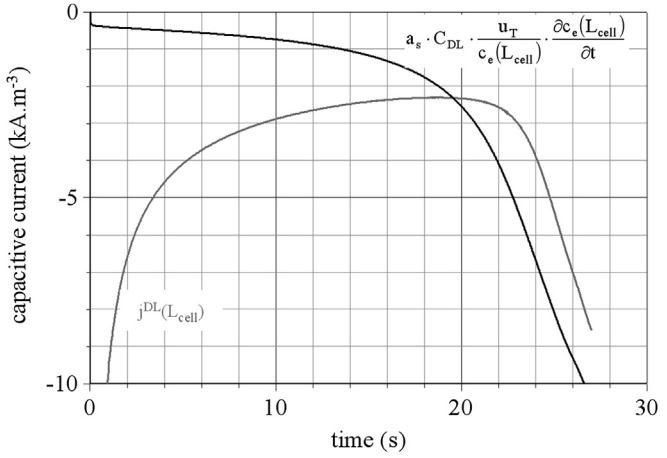

Fig. 9. Simulation of a 20 C discharge: capacitive current contributions at positive electrode terminal (electrolyte phase diffusion coefficient: $D_e = 2.6 \times 10^{-10}/10$ m^2 s^{-1}, initial SOC: 100%, temperature: 300 K).

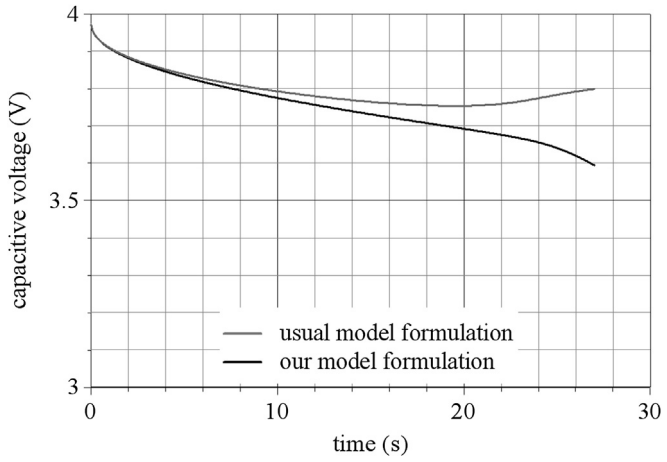

Fig. 10. Simulation of a 20 C discharge: capacitive voltage at positive electrode terminal (electrolyte phase diffusion coefficient: $D_e = 2.6 \times 10^{-10}/10$ m^2 s^{-1}, initial SOC: 100%, temperature: 300 K).

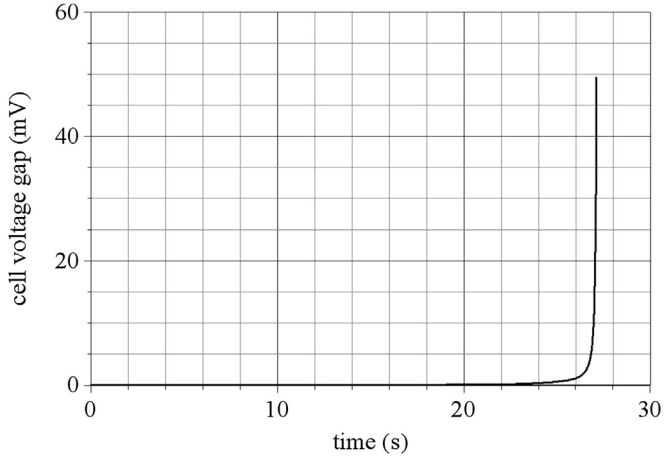

Fig. 11. Simulation of a 20 C discharge: cell voltage gap between the two formulations (electrolyte phase diffusion coefficient: $D_e = 2.6 \times 10^{-10}/10$ m^2 s^{-1}, initial SOC: 100%, temperature: 300 K).

5. Conclusion

This investigation was focused on implementing the double-layer phenomenon in the 1-D electrochemical model of lithium-ion battery cell developed in Newman's works [1] [2]. In particular, we demonstrate that the widely used formulation of this model, expressed versus an electrolyte potential defined at the average electrolyte concentration, leads to a physical error when the double layer capacitance is included. We propose an equivalent formulation of the model, expressed versus the local electrolyte concentration for electrolyte potential calculation, which enables to take into account the double layer capacitance without the physical error introduced by the usual formulation.

After these theoretical developments, we investigate the conditions for which the physical error mentioned before may cause significant inaccuracy. Equation analysis enables to determine that these conditions are met if the electrolyte concentration decreases locally down to very low values, which requires the combination of a high rate regime and a low electrolyte phase diffusion coefficient. In such conditions, simulation results show that capacitive behaviors associated with the two formulations can become locally opposite, with notably an increasing capacitive voltage during discharge, when the usual formulation is used. The cell voltage gap between the two formulations then reaches a few tens of millivolts.

References

[1] M. Doyle, T.F. Fuller, J. Newman, J. Electrochem. Soc. 140 (6) (June 1993) 1526–1533.
[2] T.F. Fuller, M. Doyle, J. Newman, J. Electrochem. Soc. 141 (1) (January 1994) 1–10.
[3] K. Smith, C.-Y. Wang, J. Power Sources 160 (1) (September 2006) 662–673.
[4] L. Cai, R.E. White, J. Power Sources 196 (14) (July 2011) 5985–5989.
[5] I.-J. Ong, J. Newman, J. Electrochem. Soc. 146 (12) (December 1999) 4360–4365.
[6] G.-A. Nazri, G. Pistoia, Lithium Batteries: Science and Technology, Kluwer Academic Publishers, Boston, 2004.
[7] K. Smith, C.-Y. Wang, J. Power Sources 161 (1) (October 2006) 628–639.
[8] S. Raël, M. Hinaje, J. Power Sources 222 (1) (January 2013) 112–122.
[9] R.B. Bird, W.E. Stewaert, E.N. Lightfoot, Transport Phenomena, second ed., Edition Wiley, New York, 2002.
[10] H.H. Girault, Electrochimie physique et analytique, deuxième édition, Presses Polytechniques et Universitaires Romandes, Lausanne, 2007, ISBN 978-2-88074-673-5.
[11] M. Doyle, J. Newman, Electrochim. Acta 40 (13–14) (October 1995) 2191–2196.
[12] K.A. Smith, C.D. Rahn, C.-Y. Wang, Energy Convers. Manage. 48 (9) (September 2007) 2565–2578.
[13] P.M. Gomadam, J.W. Weidner, R.A. Dougal, R.E. White, J. Power Sources 110 (2) (August 2002) 267–284.
[14] M.W. Verbrugge, D.R. Baker, B.J. Koch, J. Power Sources 110 (2) (August 2002) 295–309.
[15] D.M. Bernardi, J.-Y. Gob, J. Power Sources 196 (1) (January 2011) 412–427.
[16] P. Arora, M. Doyle, A.S. Gozdz, R.E. White, J. Newman, J. Power Sources 88 (2) (June 2000) 219–231.
[17] M. Doyle, J. Newman, A.S. Gozdz, C.N. Schmutz, J.-M. Tarascon, J. Electrochem. Soc. 143 (6) (June 1996) 1890–1903.
[18] J. Newman, K.E. Thomas-Alyea, Electrochemical Systems, third ed., John Wiley and Sons, New York, 2004.
[19] L.O. Valoen, J.N. Reimers, J. Electrochem. Soc. 152 (5) (May 2005) A882–A891.

Nomenclature

Latin letters

a: active surface per volume unit [m^{-1}]
A: active surface [m^2]
c: concentration [mol m^{-3}]
C_{DL}: electric double layer capacitance [F m^{-2}]
D: diffusion coefficient of species [m^2 s^{-1}]
F: Faraday's constant, 96485 [C mol^{-1}]
G^{Li}: volume rate of Li^+ generation[mol m^{-3} s^{-1}]
j_0: exchange current density [A m^{-2}]
j^{Li}: volume rate of Li^+ current generation [A m^{-3}]
j^{DL}: volume rate of double layer current generation [A m^{-3}]
J: current density [A m^{-2}]
I: current [A]
N: charge or species molar flow [mol s^{-1}]
r: radial coordinate [m]
R: radius [m]
t: time [s]
t_p: Li^+ transference number [−]
T: temperature [K]
U: electrode equilibrium potential [V]
u_T: thermal voltage [V]
V: voltage [V]
x: cartesian coordinate [m]

Greek letters

α: transfer coefficient [−]
β: Bruggeman's exponent [−]
δ: layer thickness [m]
ε: volume fraction [−]
η: surface overvoltage [V]
σ: electrical conductivity [S m^{-1}]

φ: charge or species molar flow density [mol m^{-2} s^{-1}]
ϕ: electrical potential [V]

Superscripts and subscripts

cell: battery cell
DL: double layer
e: electrolyte phase
eff: effective value
init: initial value
mean: average value
neg: negative electrode
o: oxydation
pos: positive electrode
r: reduction
s: solid phase
s,e: solid/electrolyte interface
sep: separator